Inorganic Chemistry
Article

Inorg. Chem. **2009**, *48*, 5497–5503 **5497**
DOI: 10.1021/ic900496p

Incommensurate Stistaite—Order Made to Order

S. Lidin,*,† J. Christensen,† K. Jansson,† D. Fredrickson,† R. Withers,‡ L. Norén,‡ and S. Schmid§

†*Inorganic Chemistry, Stockholm University, 106 91 Stockholm, Sweden,* ‡*Research School of Chemistry, Australian National University, Canberra, Australia, and* §*School of Chemistry, Sydney University, Australia*

Received March 12, 2009

The structure of stistaite ~SbSn, was investigated by single crystal X-ray diffraction and EDX to yield a simple relation between the modulated structure and the composition. Stistaite is found to be incommensurately ordered over the entire stability region.

Introduction

The Sn−Sb system contains two binary phases, stistaite, $Sn_{(1/2-x)}Sb_{(1/2+x)}$ that shows a relatively large existence range (ca. 40−57% Sb) Sn_3Sb_2 and a line phase that is only stable within the narrow temperature interval 250−324 °C[1] (cf. Figure 1). Stistaite, initially reported to be a rhombohedrally distorted variant of the rock salt structure type[2,3] was reinvestigated recently and shown to exhibit an incommensurate modulation.[4] There is ample evidence that Sn_3Sb_2 also is a rock-salt like structure. If crystals are grown from a Sn-rich melt below 323 °C, they exhibit a cubic habit. Quenching such crystals to room temperature produces complicated balanced twinning; the ⟨111⟩ directions of the cubic habit coincide with the *c*-axes of four different rhombohedral stistaite orientations while the ⟨100⟩ directions of the cubic habit are parallel to the tetragonal *c*-axes of elemental Sn, yielding a diffraction pattern that has overall cubic symmetry, but consist of two distinct phases with four and three different domain orientations, respectively.

It is furthermore important to note that the structure of elemental Sb itself is a rhombohedrally distorted primitive cubic structure. The distortion is caused by the formation of alternating short and long distances between the 3^6 nets of Sb atoms that are stacked along the trigonal *c*-axis direction. Locally, each Sb atom therefore has three neighbors at short distances (2.93 Å) and three neighbors at longer distances (3.38 Å).[5]

Synthesis. Six different crystals were used in this study. One was a crystal of pure Sb, from a sample produced simply by sublimation (Sample I). Four crystals (II−V) were picked from batches made by the slow growth of stistaite from melts that were first homogenized at 650 °C and then annealed for 48−96 h (Table 1). Crystals I−IV all had similar large hexagonal plate habits. The last sample was synthesized from a Sn-rich melt at 300 °C. This synthesis produced crystals of cubic habit. We assume that initially the cubic phase Sn_3Sb_2 was formed and that this subsequently transformed (unquenchably) into Sn-rich stistaite and elemental Sn. This crystal is labeled (V) in the ensuing analysis. It should be mentioned that the samples used in this study were annealed only for a few days. We have noted that long-term annealing (several months) in some cases gives rise to biphasic samples, something that was never detected in the short term annealed samples.

Compositional Analysis. The composition of the crystals used for the X-ray diffraction experiments was determined by energy dispersive X-ray spectroscopy (EDX). To achieve maximal accuracy in the analysis, the surface of the crystals was cleaned so as to remove possible remaining layers from the solidified liquid phase by use of a cross sectional polisher (Jeol, CP SM-09010). The crystals were embedded in epoxy glue, and then about 25−50 μm of them was polished away by use of a 5 kV argon ion beam to obtain a clean and parallel surface. Elemental analysis of the crystals was then performed in a scanning electron microscope (SEM, Jeol JEM 7000F) equipped with energy dispersive X-ray detector (Oxford Instruments, EDS INCA system). The X-ray radiation was generated under optimal geometric condition, with the electron beam perpendicular to the sample surface. The quantitative amount of each element was determined by use of the "XPP" algorithm,[6] included in the INCA program package.

The results of the analysis yielded the compositions given in Table 1. The data obtained agree well with a

*To whom correspondence should be addressed. E-mail: sven@inorg.su.se.

(1) *Pauling Files*; Villars, P., Ed.; NIMS: Japan, **2008**
(2) Osawa, A. *Nature* **1927**, *124*, 14.
(3) Hagg, G.; Hybinette, A. G. *Philos. Mag.* **1935**, *20*, 913–929.
(4) Norén, L.; Withers, R.; Schmid, S.; Brink, F. J.; Ting, V. *J. Solid State Chem.* **2006**, *179*, 404–412.
(5) Mozharivskyj, Y.; Pecharsky, A. O.; Bud'ko, S.; Miller, G. J. *Chem. Mater.* **2004**, *16*, 1580–1589.
(6) Pouchou, J.-L.; Pichoir, F. Quantitative analysis of homogeneous or stratified microvolumes applying the model PAP Electron Probe Quantitation. Heinrich, K. F. J., Newbury, D. E., Eds.; Plenum: New York, **1991**; pp 31−75.

Published on Web 05/14/2009

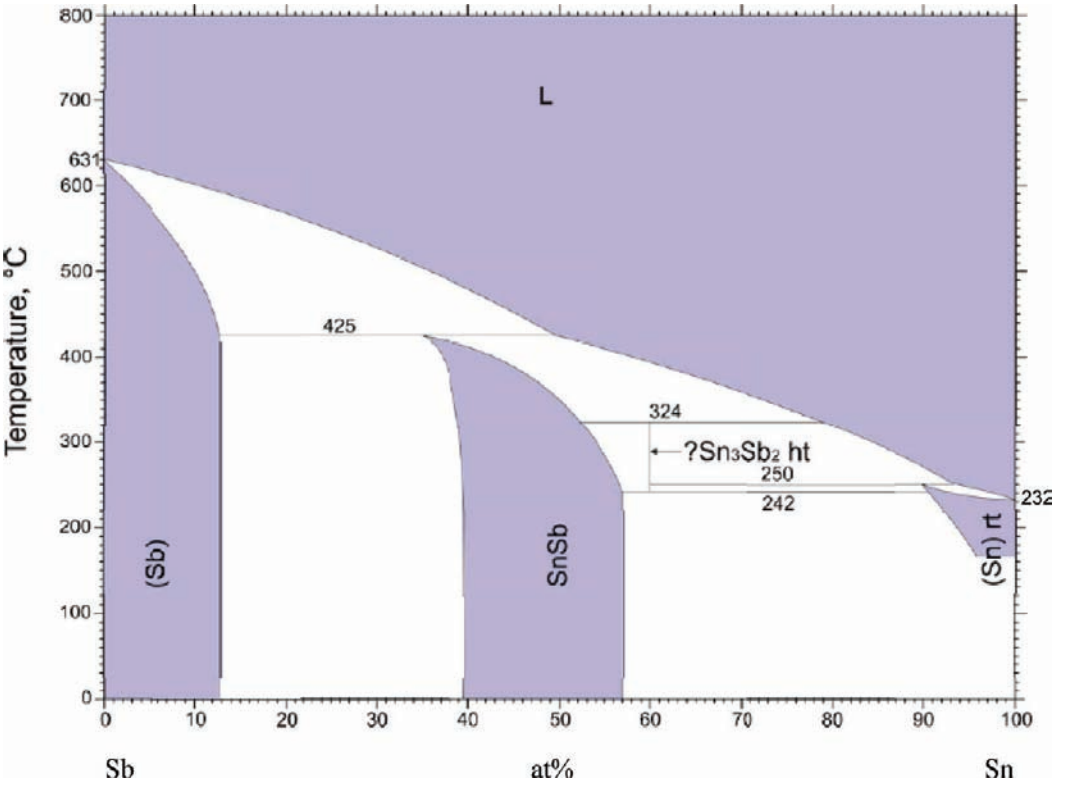

Figure 1. Phase diagram for the system Sn−Sb.

Table 1. Synthetic Protocol for Stistaite Samples II−V and Composition Determined by EDX

sample #	nominal composition	annealing temperature (°C)	at % Sn (esd)	# of EDX measurements
I	Sb			
II	Sn_9Sb_{11}	420	35.6(7)	18
III	SnSb	400	36.2(10)	14
IV	Sn_3Sb_2	350	51.4(10)	26
V	Sn_5Sb_2	260	54.1(11)	12

proposed linear relation (vide infra) between the magnitude of the incommensurate primary modulation wavevector $q = \gamma c^*$ and the Sn concentration, [Sn]. The model for the local 3-dimensional structure of stistaite depends crucially on this relation while the refinable parameters are much less sensitive. Experimental uncertainties in either [Sn] or γ are therefore not important to the interpretation as long as a linear relation between the two values is assumed. The relation is simply determined from the two end-points, so that a pure Sb sample gives the q-vector component $\gamma = 3/2$ while for the most Sn-rich sample, Sn_4Sb_3, the same parameter is given by $\gamma = 9/7$. This yields the relation $\gamma = 3/2(1 - [Sn]/4)$ and its inverse $[Sn] = 4(1 - 2\gamma/3)$. Apart from the aesthetics of simplicity, adhering to this relation also assures that the closeness condition[7] is fulfilled vide infra. The experimental relation between composition and q-vector is shown in Figure 2.

Structural Analysis. All single crystal data were measured on an Oxford diffraction Xcalibur3 system using graphite-monochromatized MoKa radiation (λ = 0.71069 Å). The data were integrated and corrected for

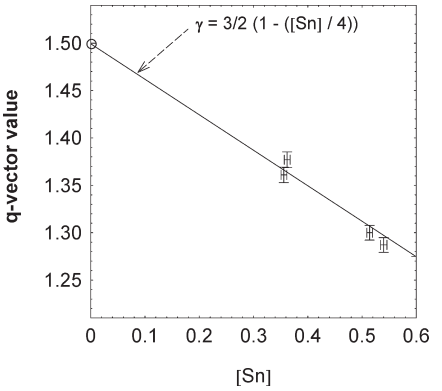

Figure 2. Relation between measured composition and q-vector component.

absorption, Lorenz and polarization effects using the ChrysalisRed software.[8] All pertinent data for the collections are given in Table 2. With the exception of Sample (V) all data sets could be indexed using a (3 + 1)d formalism. For data set (V), the data are more complex because the sample contains two phases and each of these is twinned. This measurement will be treated in more detail below. The (3 + 1)-dimensional super space group symmetry of the stistaite phase is $R\bar{3}m(00\gamma)$. The structural solution is basically a one-atom model, but the fit of the model to the data is greatly improved by modeling that single position as two separate atomic domains (Sn and Sb, respectively) and allowing for independent thermal displacement parameters and different modulation behavior for these two atomic domains. It is rather

(7) Elcoro, L.; Perez-Mato, J. M.; Darritet, J.; El Abed, A. *Acta Crystallogr.* **2003**, *B59*, 217–233.

(8) *Crysalis* software, Version 1.171.31.5, Oxford Diffraction Xcalibur CCD system; Oxford Diffraction Ltd: Oxford, U.K., **2006**.

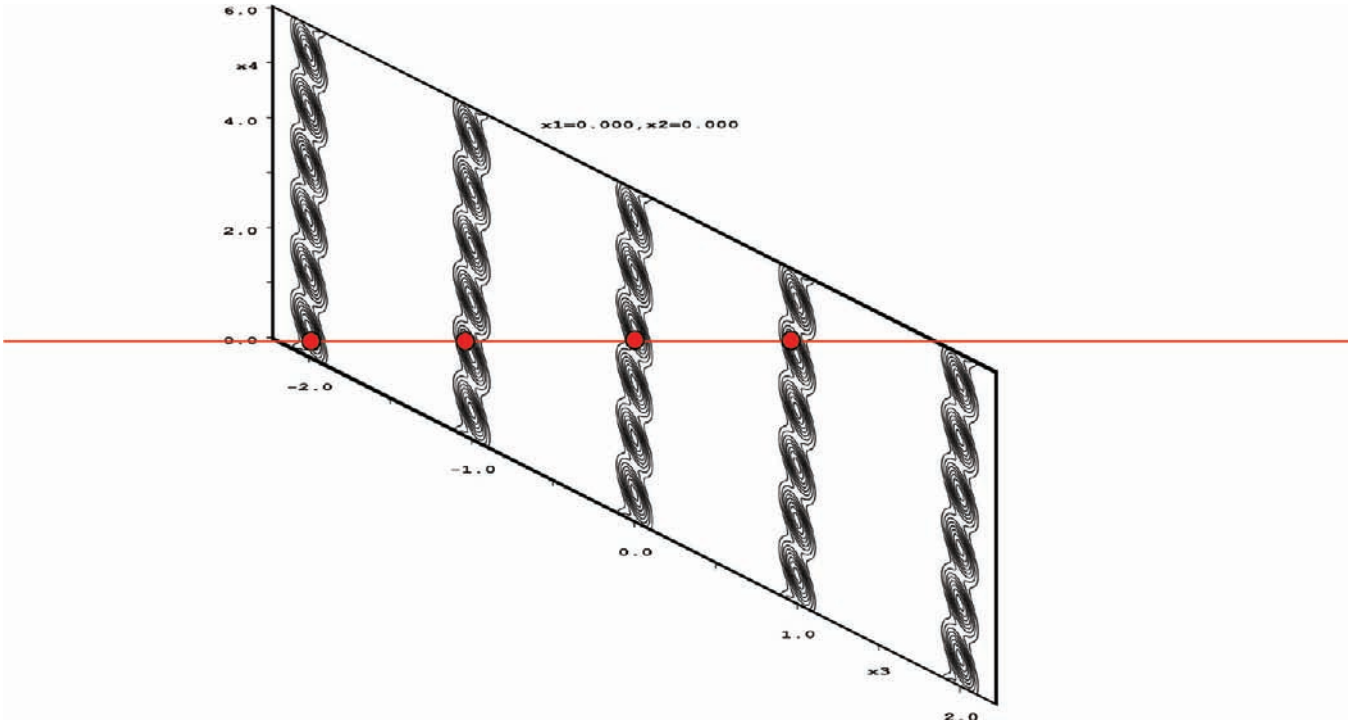

Figure 3. Electron density map from a large section of elemental Sb modeled as a commensurately modulated structure. The horizontal line represents a sampling of the modulation corresponding to physical space (*c*-axis), and the red circles represent atomic positions. Note how the out-of-step sawtooth waves generate the alternating long and short distances typical for elemental Sb.

Table 2. Data Collection for Sb and Stistaite

sample	I	II	III	IV	V
composition from model	Sb	$Sn_{0.371}Sb_{0.629}$	$Sn_{0.328}Sb_{0.672}$	$Sn_{0.576}Sb_{424}$	$Sn_{0.568}Sb_{432}$
crystal habit			hexagonal plate		cube
crystal color			silver metallic		
measurement temperature			298 K		
wavelength (Å)			0.71069, Mo Kα		
superspace group			$R3\bar{m}(00\gamma)$		
unit cell dimensions(Å)	$a=b=4.3105(3)$	$a=b=4.3071(9)$	$a=b=4.3237(15)$	$a=b=4.341(2)$	$a=b=4.291(8)$
	$c=5.6404(9)$	$c=5.3726(17)$	$c=5.4017(4)$	$c=5.323(3)$	$c=5.342(6)$
	$q=1.5$	$q=1.361(4)$	$q=1.377(2)$	$q=1.284(2)$	$q=1.287(6)$
unit cell angles(°)	90,90,120				
volume ($Å^3$)	90.760(17)	86.31(4)	87.45(4)	86.87(7)	85.20(2)
absorption coefficient (mm-1)	21.882	22.353	22.136	21.847	22.294
absorption correction			analytical from shape		
θ range for data collection(°)	5.4−48.1	5.2−34.3	5.60−33.84	5.2−44.6	4.9−37.1
	95% complete to 43	98% complete to 34	small subset	98% complete to 44.6	96% complete to 37.1
	$-8 \le h \le 8$	$-6 \le h \le 6$	$-4 \le h \le 3$	$-8 \le h \le 6$	$-7 \le h \le 7$
	$-7 \le k \le 9$	$-6 \le k \le 8$	$-6 \le k \le 3$	$-8 \le k \le 8$	$-7 \le k \le 7$
	$-11 \le l \le 10$	$-8 \le l \le 8$	$-8 \le l \le 4$	$-10 \le l \le 10$	$-9 \le l \le 9$
	$-1 \le m \le 1$	$-1 \le m \le 1$	$-1 \le m \le 1$	$-1 \le m \le 1$	$-1 \le m \le 1$
reflections collected	2317	3108	297	3003	2327
	(R_{int} = 0.03)	(R_{int} = 0.04)	(R_{int} = 0.04)	(R_{int} = 0.05)	(R_{int} = 0.06)
independent reflections	287	159	113	298	191
	($270 > 3\sigma$)	($154 > 3\sigma$)	($112 > 3\sigma$)	($274 > 3\sigma$)	($184 > 3\sigma$)
refinement method			full matrix on F^2		
data/restraints/parameters	287/0/6	159/0/7	113/0/7	298/0/7	191/0/10
final R indices [$I > 3\sigma(I)$]					
R_{main}	3.88	2.50	2.36	2.96	1.32
$R_{w,main}$	10.04	5.76	6.10	7.02	2.23
R_{sat}	2.36	2.60	2.91	3.23	7.91
$R_{w,sat}$	6.67	6.24	7.80	7.76	9.25
R indices (all data)					
R_{main}	4.31	2.50	2.36	2.96	1.32
$R_{w,main}$	10.10	5.76	6.10	7.02	2.23
R_{sat}	2.41	3.00	2.97	4.04	8.40
$R_{w,sat}$	6.68	6.31	7.80	7.82	9.30
Largest difference peak and hole	3.08/−4.86	0.74/−2.39	1.77/−0.89	1.38,−3.83	2.62,−1.65

Table 3. Structural Parameters for Sb and Stistaite

sample	I	II	III	IV	V
position Sb, Sn x,y,z			0,0,0		
[Sn]	0.00	0.37	0.328	0.576	0.568
U_{11},U_{33},U_{12} Sn		0.0209(2)	0.0216(6)	0.0195(2)	0.0150(7)
		0.021(4)	0.017(6)	0.0141(6)	0.0190(8)
		0.0104(1)	0.0108(3)	0.0098(1)	0.0075(4)
U_{11},U_{33},U_{12} Sb	0.0118(2)	0.0161(2)	0.0165(5)	0.0145(1)	0.0113(7)
	0.0219(4)	0.0185(5)	0.0138(5)	0.0139(5)	0.013(2)
	0.0059(1)	0.0080(1)	0.0083(2)	0.0072(1)	0.0056(3)
Sinz1, Sinz2	*-0.0149(7)*	0.0269(1)	0.0287(2)	0.02446(12)	0.021(3)
	Sawtooth	0.012(2)	0.0144)	0.0074(8)	

unexpected that this should be the case, since the contrast between the neighboring Sb and Sn should be weak using X-rays with energy far away from the absorption edge of both elements. As we understand it, this indicates that the two elements behave quite differently in the structure, Sb forming a stiff substructure and Sn a soft one. This behavior provides the refinement with the bonus of a stronger contrast between Sn and Sb than expected. Thus, we arrive at a model where the Sn and Sb positions are distinct, that is, Sn and Sb will be modeled using square-wave type occupancy domains, or to put it simply, an on/off function. The atoms are either Sn or Sb, and we do not need to consider mixed sites. The alternation between Sb and Sn is of course what makes this a NaCl type structure rather than an α-Po type structure, and NaCl itself may be modeled as an occupationally modulated α-Po type structure. Further, we find that the positional modulation changes with the Sb content. Modeling elemental Sb (sample I), containing alternating short and long interlayer distances, we use a highly non-harmonic sawtooth wave. For Sb-rich stistaite (samples II−IV) the displacement function is better modeled using harmonic functions, but requires second order harmonics to provide a satisfactory fit, while for Sn-rich stistaite (sample V) a single harmonic wave is enough. To interpret the modulated model, it is useful to consider the physical space section through the formal (3 + 1)-dimensional description used. In Figure 3 this is shown for elemental Sb. Note how sampling the modulation function along the horizontal direction representing physical space generates alternating long and short distances between successive atomic layers along c. For the more harmonic cases of samples II−V, the corresponding alternation becomes less pronounced with increasing Sn content. The parameters of the refined models are given in Table 3. An alternative, single atom model, with modulated thermal displacement parameters yields equally satisfactory results in terms of fit to the data. Such a model emphasizes the similarity of Sb and Sn in the NaCl type blocks, and this similarity might explain the failure of previous studies to observe satellites in the HT-phase Sn_3Sb_2. This model, however, fails to address the observed relation between composition and the magnitude of the primary modulation wave vector.

Sample (I). Pure Sb may be described as a commensurately modulated structure with a basic structure containing one atom in the unit cell, and a q vector of $(0,0,\gamma)$, $\gamma = 3/2$, compare Figure 4a. The advantage of such a description is that it highlights the underlying feature of the structure as a simple periodic distortion of a

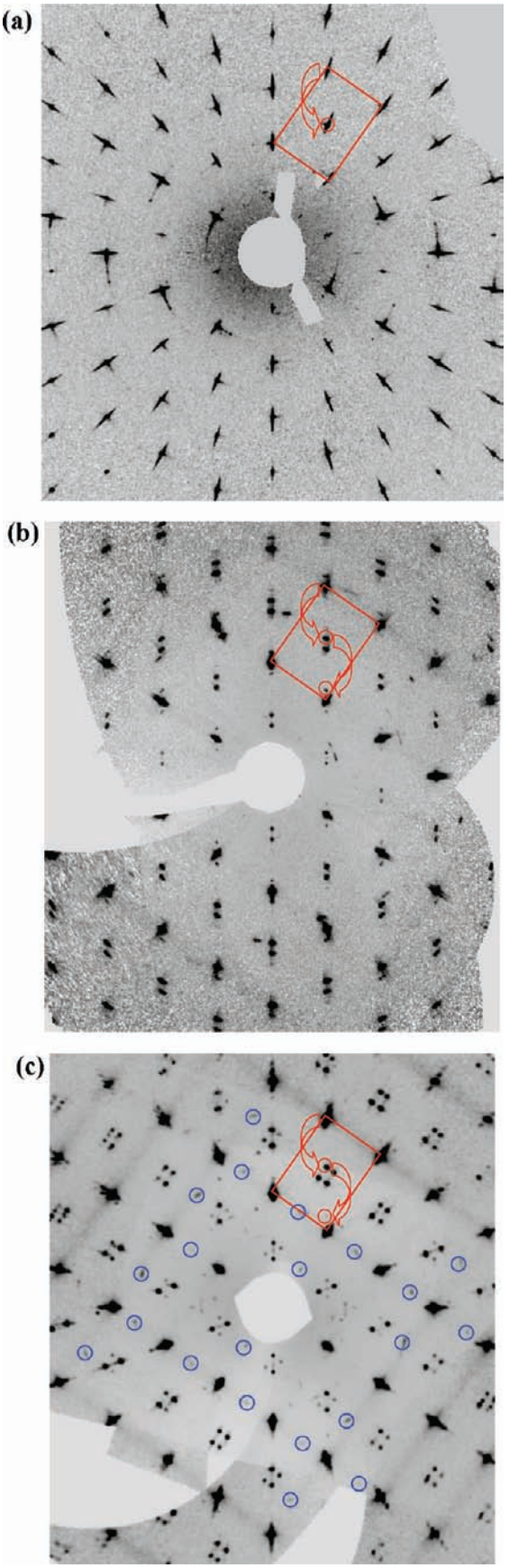

Figure 4. (a) Diffraction pattern of pure Sb (sample I); (b) diffraction pattern for Sb-rich stistaite (sample II); (c) diffraction pattern for twinned, Sn rich, stistaite (sample V). Diffraction from elemental Sn indicated as blue circles.

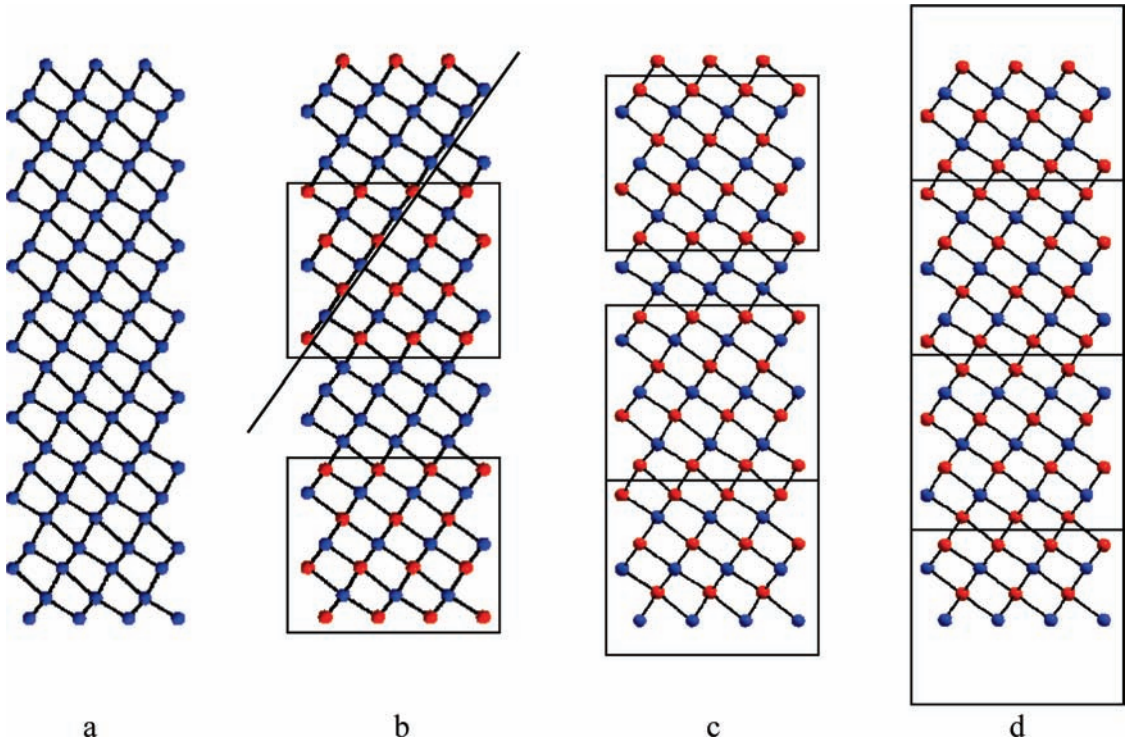

Figure 5. Structures of modulated stistaite and elemental Sb shown in projection down *a*. The *c*-axis is vertical. Sb atoms are shown in blue, Sn in red. Note that all structures are basically colored versions of α-Po. (a) Sample I, elemental Sb. (b) Sb-rich stistaite, ~Sb2Sn sample II. Note how the Sb part of the structure displays a clear zigzag shape along the diagonal, whereas the NaCl type block is much flatter. (c) ~SbSn, sample IV. (d) Sn-rich stistaite Sb3Sn4, sample V.

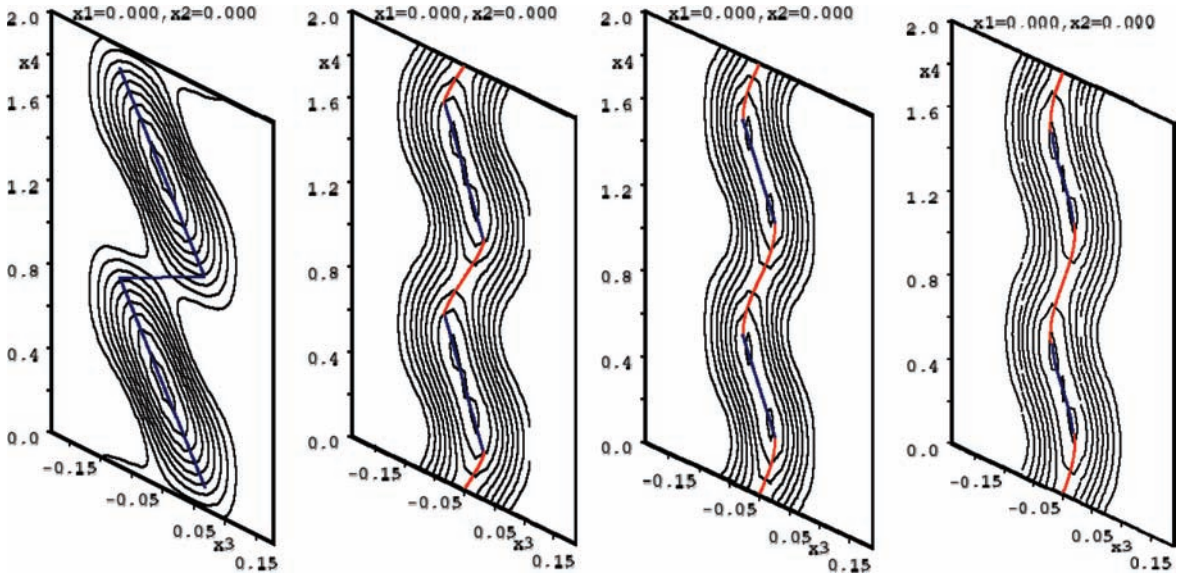

Figure 6. Electron density maps of the modulated structures of samples I (a), II (b), IV (c), and V (d).

primitive cubic parent structure. It also leads to a structural model that is congruent with that of stistaite. The structure of Sb is well understood in terms of a standard covalent bonding model. Sb, having five valence electrons and requiring three bonds to complete an octet, will deform along the (111) direction of the primitive cubic structure in a manner that leads to alternating short and long distances between adjacent 3^6 nets of Sb atoms (cf. Figure 5a). In a commensurately modulated model this is simply modeled as a sawtooth like displacement along *c* (cf. Figure 6a).

Samples II−III. If the Sn content of a Sb sample is increased beyond the solubility limit, a new phase forms: stistaite. Stistaite has a maximum Sb content of about 64% in our experiments {Sample II: 64.4(7), Sample III: 63.8(10)} but the compositional boundaries of the phase may well vary with temperature. In the diffraction pattern of Figure 3b the Sb-rich limit of the phase exhibits a clearly incommensurate behavior. The single satellite reflection at $\gamma = 1.5$ of the Sb phase is replaced by a pair of intense satellite reflections straddling that position with $\gamma \approx 1.36$ {Sample II: 1.36, Sample III: 1.37}.

A relatively large number of second order satellite reflections are visible in the close vicinity of the main reflections, and in some places it is possible to see even third order satellite reflections. This is an indication of an anharmonic modulation with high amplitude. The structure consists of two kinds of blocks. In one of these, rather equidistant layers of Sb and Sn alternate to form stacks of seven layers terminated by Sn. This block is indicated in Figure 5. Technically this block is a slab of NaCl structure type. The other type of block is elemental Sb in which the native pairing of adjacent layers is preserved. This description is clearly a simplification as the two blocks intergrow seamlessly, but it is qualitatively correct as can be seen by following a diagonal row of atoms as indicated in Figure 5b. The row is relatively straight at the center of the NaCl block, while it follows a zigzag line in the Sb block. The electron density corresponding to the Sb atom is best modeled by a sawtooth function, while that of Sn is best modeled by a simple harmonic wave. The details of the single crystal X-ray refinement are given in Table 2.

Sample IV. For more Sn rich samples, the diffraction patterns change in two distinct ways. First, the magnitude of the q vector shortens, and second, the satellite reflections grow less intense. This second effect is best seen by observing the higher order satellite reflections. For Sample IV, the second order satellite reflections are far less numerous, while the third order satellite reflections are missing altogether. The Sb content of phase IV is 51.4(10)% while the primary modulation wave vector magnitude is $\gamma = 1.300$. The reason for this behavior is the decrease in modulation amplitude, as well as the more harmonic shape of the modulation. This can be seen in the refined structure shown in Figure 5c, and from the electron density in Figure 6c. The Sn-terminated NaCl structure blocks alternate with double layers of Sb. The best model uses harmonic functions for Sn and Sb alike, cf. Table 3.

Sample V. Sample V was made in a different way from the other samples in this series. Being formed by the (unquenchable) peritectic decomposition of the cubic high temperature phase Sn_3Sb_2, it contains excess Sn, and the stistaite is twinned to mimic the cubic symmetry of the parent phase, the *c*-axes of the four different allowed domain orientations coinciding with the body diagonals of the cubic habit of the outer shape of the crystals. As a result, it has a distinct, and very complex, X-ray diffraction pattern (Figure 4c). Apart from the reflections stemming from the obvious twinning of the stistaite, a careful inspection also reveals reflections from β-Sn crystallites. These are aligned with their unique *c*-axes parallel to the axial directions of the external crystal shape to yield an interesting composite diffraction pattern. Finally, the diffraction pattern contains noticeable structured diffuse scattering of the kind observed previously for twinned stistaite samples.[2] Even more remarkable than the unquenchable nature of the transformation from the high temperature phase is the room temperature behavior of this composite sample. Storing this sample a few months yields a single domain stistaite sample with much reduced diffuse contributions, and no measurable (by X-ray diffraction) content of Sn. The stistaite structure in Sample V is refinable using the same model as for the other samples (and taking twinning into account), but naturally, the data appear less dependable given the complex overlap pattern.

Results and Discussion

The local behavior of this structural family may be explained in a straightforward way, starting from the structure of elemental Sb: layers of Sn intercalate the Wan der Vaals' gap between Sb double layers. This destabilizes the Sb−Sb bonding between the neighboring layers and favors intercalation of subsequent Sn layers to form alternating Sb/Sn seven-layer stacks terminated by Sn. For relatively limited amounts of Sn, this leads to solid solutions. While it is probable that seven-layer stacks are stable also at relatively low Sn concentrations, the average distance between such stacks is large, and therefore no long-range order is observed. In fact, at 10 at % Sn in Sb (the limit of solid solubility is ca. 13%) the average separation between seven-layer stacks would be 33 layers of Sb. As the amount of Sb in the blocks separating seven-layer stacks decreases, the tendency toward ordering will increase. At 36% Sn the stable homogeneous phase consists of alternating blocks of Sb_4 and Sn_4Sb_3. This Sb-rich stistaite is characterized by satellite reflections of relatively high intensity. As the Sn content increases, the overall tendency toward covalent bonding decreases, the Sb_4blocks are replaced by Sb_2-blocks, or disappear all together, and the sawtooth like behavior of the positional modulation function is replaced by a more harmonic function with a smaller amplitude. For the most Sn rich phase, Sn_4Sb_3, there are no Sb_2 blocks at all, but the structure consists entirely of seven-layer stacks of Sn_4Sb_3 as shown in Figure 5d.

There is no paucity of super-structured, rock-salt type main group compounds, and their ordering behaviors are quite diverse. Compounds such as As_2Te_3 are basically stoichiometric, containing the expected five-layer rock-salt blocks, while the ternary $As_2Ge_nTe_{3+n}$ form long blocks corresponding to the total composition.[9] In the Sb−Te system, we find five-layer blocks of Te_3Sb_2 alternating with blocks of pure Sb,[10] and the systems Bi−Te and Bi−Se display extensive, incommensurately ordered, solid solution domains between the compositions Bi_2X_3 and Bi_4X_3. In these latter systems, Bi_2-bilayers are regularly intercalated between five-layer blocks of Bi_2X_3 to form the structure.[11,12]

In elemental Sb the q-vector is $(0,0,\gamma)$, $\gamma = 3/2$ and γ decreases monotonically with increasing Sn content according to $\gamma = 3/2(1 - [Sn]/4)$ where [Sn] is the relative content of tin in the phase. This relation agrees with the observed relation between composition and γ, but the exact formulation is based on a mechanism wherein the seven-layer-block that builds the Sn richest phase Sn_4Sb_3 is retained throughout the series, and the increase in Sb content is achieved through the interleaving of additional layers of Sb_{2n}. This description disregards the miscibility gap between stistaite and elemental Sb, but it may be argued that this miscibility gap is simply caused by correlations becoming ineffective at large distances. Let us consider a very Sn-poor sample, such as the limiting case for solid solubility of Sn in Sb, that is, about

(9) Shu, H. W.; Jaulmes, S.; Flahaut, J. *J. Solid State Chem.* **1988**, *74*, 277–286.
(10) Kifune, K.; Kubota, Y.; Matsunaga, T.; Yamada, N. *Acta Crystallogr.* **2005**, *B61*, 492–497.
(11) Lind, H.; Lidin, S. *Solid State Sci.* **2003**, *5*(1), 47–57.
(12) Lind, H.; Lidin, S.; Haussermann, U. *Phys. Rev.* **2005**, *B72*, 184101.

10%. For an ordered case, this would correspond to Sn_4Sb_3 seven-blocks alternating with Sb-blocks 33 Sb-layers thick. It is unsurprising that such dilute systems do not order. For Sn richer cases, the samples will phase-separate into Sb-rich stistaite ($\sim SnSb_2$) and Sn-rich Sb.

A second, less obvious effect is the fall-off in intensity of the satellite reflections with increasing Sn content. The reason for this is straightforward. As Sn replaces Sb, the strict alternation of long and short distances between adjacent layers is gradually softened. This is very clearly seen in the atomic modulation function that goes from a strict sawtooth shape for elemental Sb to a much more sinusoidal shape for the high Sn content stistaite. A simple interpretation of this is that the introduction of Sn, with the accompanying lowering of the electron count, favors a higher degree of bonding. The limiting case for this process would be a compound with the composition Sn_3Sb_2 that may be treated as a salt with the formal charges $(Sn^{2+})_3(Sb^{3-})_2$. Although the charges are entirely formal, the interesting point is that this structure should be characterized by uniform octahedral coordination for all atoms.

This brings us back to the enigmatic nature of the real compound Sn_3Sb_2. The similarity of the scattering factors of Sn and Sb, combined with the expected homogeneity of distances in a NaCl type compound of the two, would explain the failure to recognize any super structure ordering in a powder diffraction pattern. The strong evidence for a cubic structure further corroborates this; if the structure of Sn_3Sb_2 is indeed cubic, and exhibits Sn−Sb ordering (as suggested by the non-quenchable transformation to a highly ordered, albeit twinned, stistaite) any superstructure reflections will be symmetry-diluted, that is, spread out over many symmetry equivalent positions in reciprocal space, while the reflections from the underlying, simple cubic structure will be very strong. This controversy can best be resolved by a high temperature, single crystal X-ray or neutron study.

Acknowledgment. This research was supported by Swedish Research Council (S.L.) and the EU network CMA (D.F.). We further acknowledge the Knut and Alice Wallenberg foundation for financing the electron microscopes used.